**Geomechanics and Engineering**, *Vol. 7, No. 2 (2014) 165-181*
DOI: http://dx.doi.org/10.12989/gae.2014.7.2.165 

# Experimental and numerical investigation of uplift behavior of umbrella-shaped ground anchor

Hong-Hu Zhu [1a], Guo-Xiong Mei [*2], Min Xu [2b], Yi Liu [2c] and Jian-Hua Yin [3d]

[1] *School of Earth Sciences and Engineering, Nanjing University, Nanjing, China*
[2] *College of Transportation Science and Engineering, Nanjing Tech University, Nanjing, China*
[3] *Department of Civil and Environmental Engineering, The Hong Kong Polytechnic University, Hong Kong, China*

(*Received August 08, 2013, Revised March 31, 2014, Accepted April 12, 2014*)

**Abstract.** In the past decade, different types of underreamed ground anchors have been developed for substructures requiring uplift resistance. This article introduces a new type of umbrella-shaped anchor. The uplift behavior of this ground anchor in clay is studied through a series of laboratory and field uplift tests. The test results show that the umbrella-shaped anchor has higher uplift capacity than conventional anchors. The failure mode of the umbrella-shaped anchor in a large embedment depth can be characterized by an arc failure surface and the dimension of the plastic zone depends on the anchor diameter. The anchor diameter and embedment depth have significant influence on the uplift behavior. A finite element model is established to simulate the pullout of the ground anchor. A parametric study using this model is conducted to study the effects of the elastic modulus, cohesion, and friction angle of soils on the load-displacement relationship of the ground anchor. It is found that the larger the elastic modulus and the shear strength parameters, the higher the uplift capacity of the ground anchor. It is suggested that in engineering design, the soil with stiffer modulus and higher shear strength should be selected as the bearing stratum of this type of anchor.

**Keywords:** umbrella-shaped anchor; pullout behavior; uplift test; numerical analysis; uplift capacity

## 1. Introduction

With the increase of massive underground and offshore construction activities, the utilization of an efficient and reliable anchorage system for buoyant foundations has attracted a lot of attention. In recent years, different types of anchors and piles have been developed for substructures requiring uplift resistance. There are basically three types of anchors, i.e., plate anchors, helical anchors and grouted anchors. The primary function of these anchors is to transmit pullout forces to the ground soil. In the past few decades, the uplift behavior of various types of anchors in sand and clay has been studied by a number of experimental and theoretical researches.

*Corresponding author, Professor, E-mail: meiguox@163.com
[a] Associate Professor, E-mail: zhh@nju.edu.cn
[b] Master Student, E-mail: xm_fly@163.com
[c] Master Student, E-mail: liuyi1982_61@126.com
[d] Professor, E-mail: cejhyin@polyu.edu.hk


http://www.techno-press.org/?journal=gae&subpage=7 ISSN: 2005-307X (Print), 2092-6219 (Online)

In the past few decades, the pullout behavior of anchors and soil nails embedded in soil masses have been investigated through numerous experimental and theoretical studies (e.g., Matsuo 1967, 1968, Hsu and Liao 1998, Huang *et al*. 2011, Zhou and Yin 2008, Zhou *et al*. 2011, 2013, Yin and Zhou 2009, Zhu *et al*. 2011, Hong *et al*. 2012, 2013a, 2013b, Zhang *et al*. 2014). The uplift capacity and failure mechanism of round anchor is found to be highly dependent on anchor shape, embedment ratio, and soil properties (Kame *et al*. 2012, Liu *et al*. 2013, Consoli *et al*. 2013, Niroumand and Kassim 2013). The anchors with a strip, square, circular, or rectangular shape are found to show different response under uplift loading (Rowe and Davis 1982a, b). Merifield *et al*. (2003) quantified the effect of anchor shape on the ultimate pullout capacity using three-dimensional limit analysis method. The rigorous lower bound solutions for the ultimate capacity of square, circular, and rectangular anchors in clay are derived. More recently, an empirical relationship is proposed by Singh and Ramaswamy (2008) for determining the shape factor and loading capacity of plate anchors in soft soil. Ilamparuthi *et al*. (2002) demonstrated the differences in failure modes between shallow and deep circular plate anchors in sand through a series of laboratory model tests. For cylindrical anchors in sand, a critical depth is proposed by Hsu and Liao (1998) to differentiate a deeply embedded anchor from an anchor with shallow embedment. Regarding the failure pattern of uplifted anchors or footings, Matsuo (1967, 1968) proposed a logarithmic spiral and a plane rupture surface. In the theoretical analyses of Murray and Geddes (1987), the curved failure surface obtained from a series of laboratory uplift test is simplified as a plane rupture surface. On the contrary, Ghaly and Hanna (1994) claimed that a logarithmic spiral surface can be used in limit equilibrium analyses of screw anchors. The group effect of closely placed anchors under pullout loading is investigated by Bhattacharya and Kumar (2013). Their numerical analyses indicate that the anchor spacing, soil unit weight, and embedment ratio have significant influence on the pullout capacity of horizontal anchor plates.

In certain cases, a large anti-float force is required for ground anchors with a fixed anchorage length. The commonly used approaches are to improve the grouting quality, reinforce the soil mass, or to enlarge the anchor head. With respect to the last method, the shear strength of soil around the anchor head and the weight of anchor head and soil it contains will be increased so that a higher pullout capacity can be obtained. Liao and Hsu (2003) introduced a new blade-underreamed anchor and studied the anchorage mechanism of this anchor through full-scale uplift tests and numerical simulation. This anchor is found to have a higher pullout capacity than that of a straight shaft anchor. Zhang (2006) reported the development of an innovative umbrella-shaped (US) self-expanding anchor for soil reinforcement and successfully applied these anchors to support an excavation in Shanghai, China. The field monitoring results verify the effectiveness of this anchor to reduce the deformation of the excavation.

In this article, the effectiveness of this novel US ground anchor, which was first advocated by Zhang (2006), for providing a foundation with anti-float force is estimated. Through a series of laboratory and field uplift tests, the uplift performance of this ground anchor is investigated. Afterward, some factors influencing the uplift behavior of this type of anchor are investigated based on the results of finite element analyses.

## 2. Development of the US ground anchor

The structural design of this anchor was done with consideration of the convenience of site maneuvering and the requirement of structural strength. The structure diagram of a US ground

DKSLDUanchor is shown in Fig. 1. The anchor is made of stainless steel and consists of two sliding sleeves, a locking ring, a supporting shaft, several stretchers and outwardly extending ribs (Liu *et al*. 2009). Fixed connections are provided between the upper sleeve and the upper plate, as well as the lower sleeve and the lower plate. The locking ring is welded to the upper sleeve. The upper plate and sliding shaft, the lower plate and the extending ribs, and sliding shaft and the extending rib are connected by hinges. Each supporting rod is connected with two wing members through a bolt. The dimensions of the structural components are listed in Table 1.

The installation of the US ground anchor is illustrated in Fig. 2. First, a borehole with a predetermined diameter and a predetermined length will be prepared. The closed anchor will be inserted into the borehole. The shaft will be fixed as the counterforce device and the upper plate will be pushed down using a steel tube placed on it. The stretchers and extending ribs will cut the surrounding soil mass and the anchor head will be gradually opened. Then the borehole will be backfilled with crushed stones or compacted soil so that an umbrella-shaped anchor will be constructed. Normally, pressure grouting of the anchor head using cement slurry will be applied

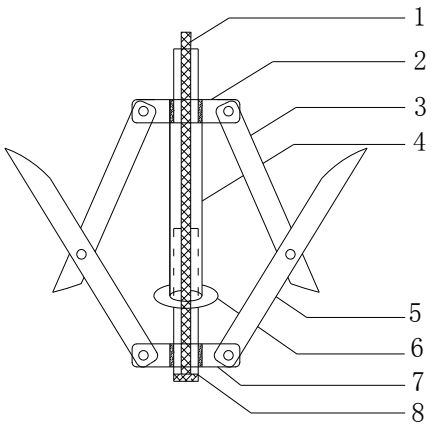


Fig. 1 Structure diagram of the US ground anchor (adopted from Liu *et al*. 2009): 1 - Supporting shaft (steel bar or steel wire rope); 2 - Upper plate; 3 - Stretcher; 4 - Upper sleeve; 5 - Outwardly extending rib; 6 - Locking ring; 7 - Lower plate; 8 - Lower sleeve

Table 1 Dimension of the US ground anchor

| Element of anchor | Number of elements | Length (mm) | Width (mm) | Thickness (mm) | Diameter (mm) |
|---|---|---|---|---|---|
| Supporting shaft | 2 | — | — | — | 12 |
| Upper plate | 1 | — | — | 24 | 120 |
| Supporting rod | 6 | 200 | 24 | 5 | — |
| Upper sleeve | 1 | 340 | — | 2 | 34 |
| Outwardly extending rib | 12 | 350 | 24 | 5 | — |
| Locking ring | 1 | — | — | 8 | 65 |
| Lower plate | 1 | — | — | 24 | 120 |
| Lower sleeve | 1 | 380 | — | 2 | 26 |

during the anchor installation works. As shown in Fig. 3, an excavated anchor showed an underream body with an irregular shape. The average diameter $D$ of cement grouting of the anchor is 670 mm. As a result, the load transfer mechanism of this anchor will be different from that of conventional shaft or plate anchors.

## 3. Laboratory uplift tests on the US anchors

To evaluate the anchorage behavior of the US anchor and the effect of grouting, laboratory uplift tests were performed on three types of shallow anchors, including cement grouted

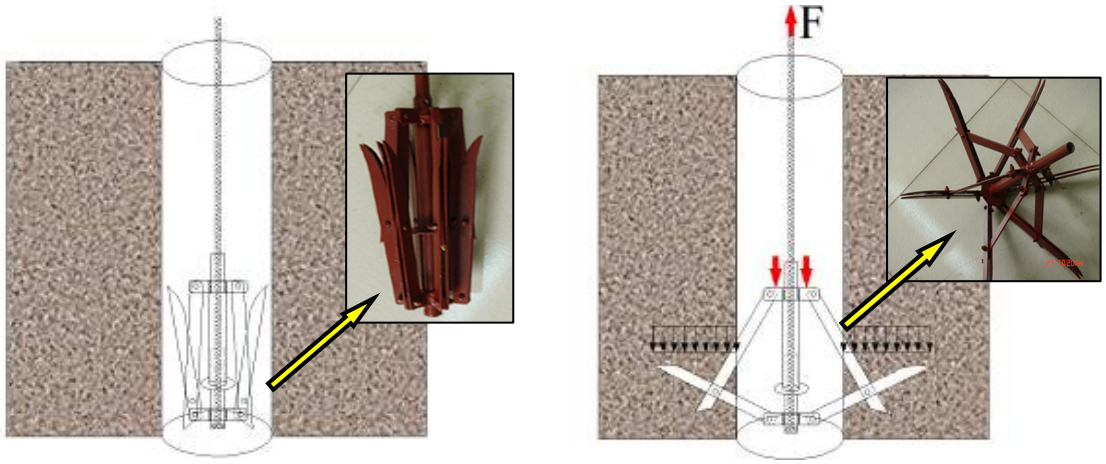


(a) Before opening (b) After opening

Fig. 2 Installation diagram of the US anchor

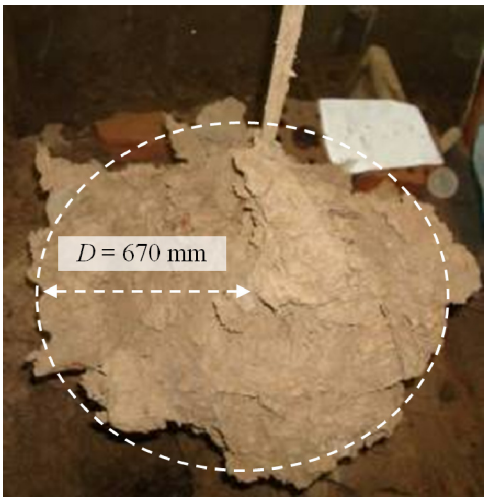


Fig. 3 Photograph of the excavated US anchor

conventional cylindrical anchors with a diameter of 160 mm, US anchors without grouting, and US anchors with pressure grouting (Xu *et al*. 2009). The embedment depths of these anchors were kept as 1 m.

The physical and mechanical properties of the silty clay used in the tests are mentioned in Fig. 4 and Table 2. The shear strength parameters were obtained from triaxial compression tests (consolidated undrained). As shown in Fig. 5, the anchors were installed in a 3.0 m × 2.0 m × 1.0 m test chamber. The test soil was laid out in series of horizontal layers with a thickness of 100 mm. Each layer was tamped equally with a tamping rod to obtain the prescribed height. Afterward, a borehole was drilled in the ground. During the installation of US anchors, the boreholes were backfilled and the cement slurry of 0.5 water cement ratio were used as the grouting material. For the US anchors with pressure grouting, the initial grouting pressure is 0.3-0.5 MPa. After two hours' setting, a secondary grouting with a pressure of 0.8-1.0 MPa was applied. The uplift tests were conducted twenty days after backfilling the borehole.

During testing, the pullout load was applied on the anchor top in stages using a hand chain hoist. The loads and displacements were measured by a load cell of 0.01 kN sensitivity and a dial gauge of 0.01 mm sensitivity, respectively. The loading rate was about 5 mm/min. A total of nine pullout tests were carried out. Figs. 6 and 7 depict the typical test results and corresponding failure patterns of the ground surface, respectively.

For the cylindrical anchors, the pullout load increased gradually up to 3.8 kN after 93 mm uplift displacement. It is found that the failure occurred apparently at the soil-anchor interface, indicating that the uplift capacity mainly depends on the shaft friction. There was no significant heave of

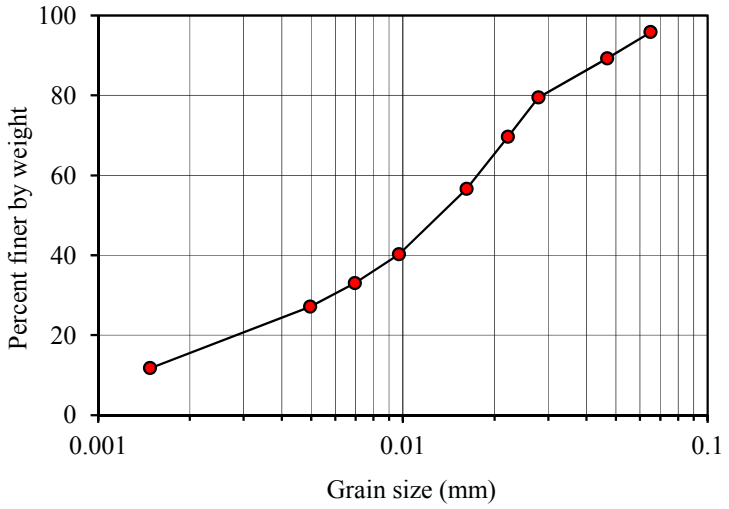


Fig. 4 Particle size distribution of the silty clay used in the laboratory uplift tests

Table 2 Properties of the silty clay used in the laboratory uplift tests

| Unit weight $\gamma$ (kN/m$^3$) | Water content $w$ (%) | Specific gravity $G_s$ | Void ratio $e$ | Plastic index $I_P$ (%) | Liquidity index $I_L$ | Cohesion (kPa) | Friction angle (°) |
|---|---|---|---|---|---|---|---|
| 18.0 | 40.2 | 2.74 | 1.10 | 17.4 | 1.0 | 5.0 | 20.0 |

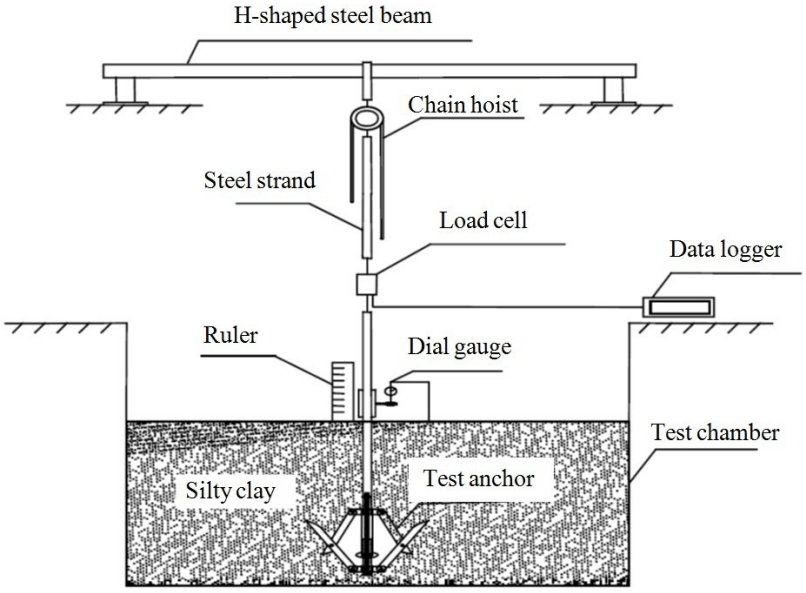


Fig. 5 Setup of a laboratory uplift test (adopted from Liu *et al*. 2009)

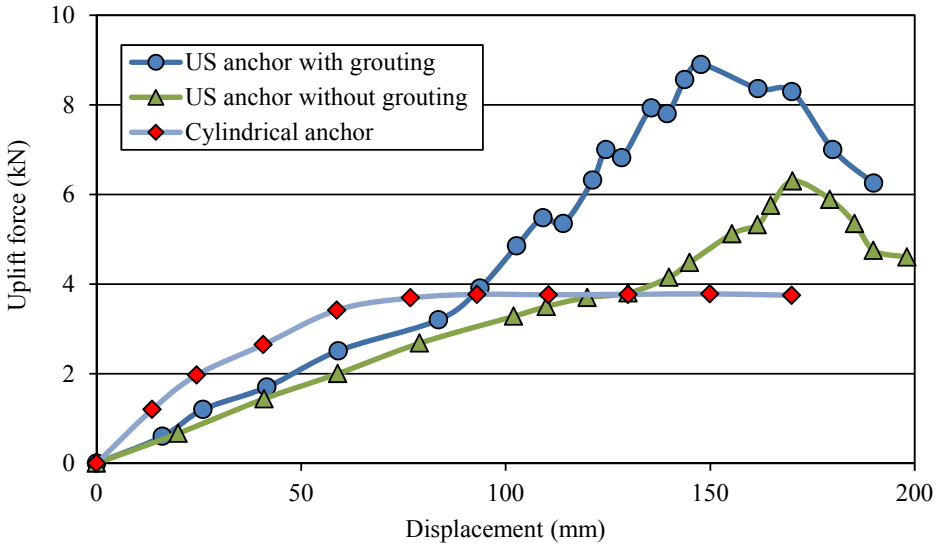


Fig. 6 Relationship between uplift force and displacement in the laboratory uplift tests

ground soil according to observations. The load-displacement relationship approximately follows a hyperbolic function.

For the US anchors without grouting, at the initial stage, the uplift displacement was small and the pullout resistance was mainly balanced by the weight of soil. Small cracks gradually appeared and propagated on the soil surface with the increase of loading. As the cross-sectional area of the non-grouted anchor was small, the stretchers and extending ribs of the uplifted anchor cut the soil

mass like blades. While the uplift load increased, the relative displacement between the soil and the anchor developed accordingly, and ultimately, the anchor were uplifted outside the soil masses through the cracks. The ground surface above the anchor was seen to bulge upwards to several centimeters. The ultimate uplift capacity of the umbrella-shaped anchors without grouting is about 6.2 kN. From the above observations, it can be concluded that both the weight of soil mass that the anchor head contains and the friction between the stretchers and extending ribs and soil play important roles in resisting the uplift loading.

For the US anchors with pressure grouting, it is noticed that the crack lengths on the ground surface are much greater compared with those without grouting. Although the distribution of cracks was similar to that of the extending ribs, there were significant ground heave during the uplift process of the umbrella-shaped anchors with grouting. The measured ultimate uplift capacity is about 8.9 kN. It is indicated that both the whole weight of anchor-soil mass and the soil shear

(a) Cylindrical anchor

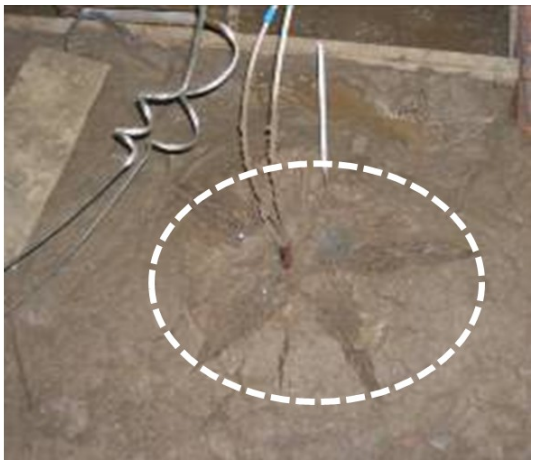

(b) US anchor without grouting

(c) US anchor with grouting

Fig. 7 Failure patterns of the ground surface after the laboratory uplift tests

strength contribute to the uplift capacity. The grouting process provides the anchor with a larger anchorage regime and hence a much higher uplift capacity. The load-displacement curves of shallow US anchors with and without pressure grouting are similar, but the peak pullout resistance of the pressure grouted US anchor is drastically higher than that without pressure grouting.

## 4. Field uplift tests on the US anchors

In the laboratory uplift tests, the embedment depth $H$ of the US anchor was only 1 m (embedment ratio $H/D$ = 1.5). To evaluate the uplift behavior of deeply embedded US anchor, a series of field uplift tests were carried out in this study. The field tests were conducted at a construction site in Ningbo, Zhejiang Province, China. The physical and mechanical properties of soils are listed in Table 3. Before the uplift tests, a trial was conducted to ensure the field installation quality of the US anchor. It is shown in Fig. 8 that the anchor diameter was 670 mm, indicating the excavated anchor head had been completely opened.

Fig. 9 depicts the setup of the in-situ uplift tests. A hydraulic jack rested on the reaction frame was utilized to apply the uplift loading. The uplift force was calculated from the pressure gauge fixed on the hydraulic jack. The uplift displacement was measured by a digital dial gauge of 0.01 mm sensitivity. The loading rate was the same as that of the laboratory uplift tests. Fig. 10 shows

Table 3 Properties of the soils used in the field uplift tests

| No. | Soil type | Thickness (m) | Unit weight $\gamma$ (kN/m$^3$) | Water content $w$ (%) | Void ratio $e$ | Cohesion $c$ (kPa) | Friction angle $\varphi$ (°) |
|---|---|---|---|---|---|---|---|
| 1 | Fill | 3.5 | 20.0 | - | - | 3.0 | 30.0 |
| 2 | Silty clay | 22.0 | 17.5 | 32.0 | 0.92 | 8.0 | 10.0 |

Fig. 8 Photograph of an excavated US anchor in the field

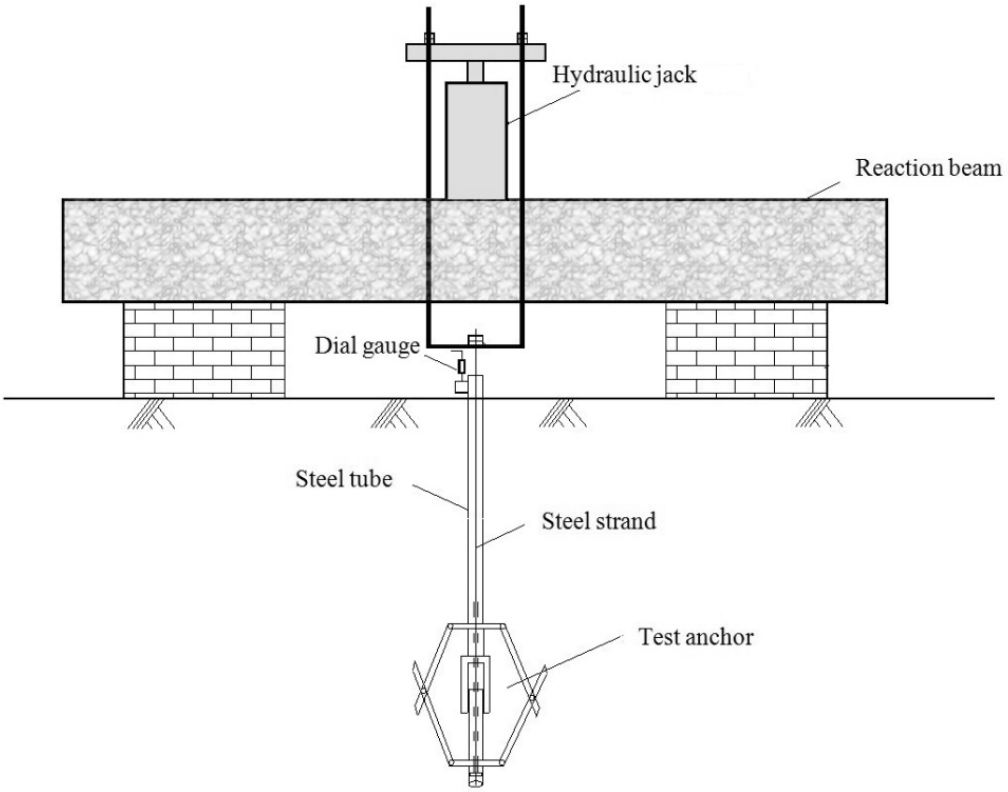


Fig. 9 Setup of the field uplift tests

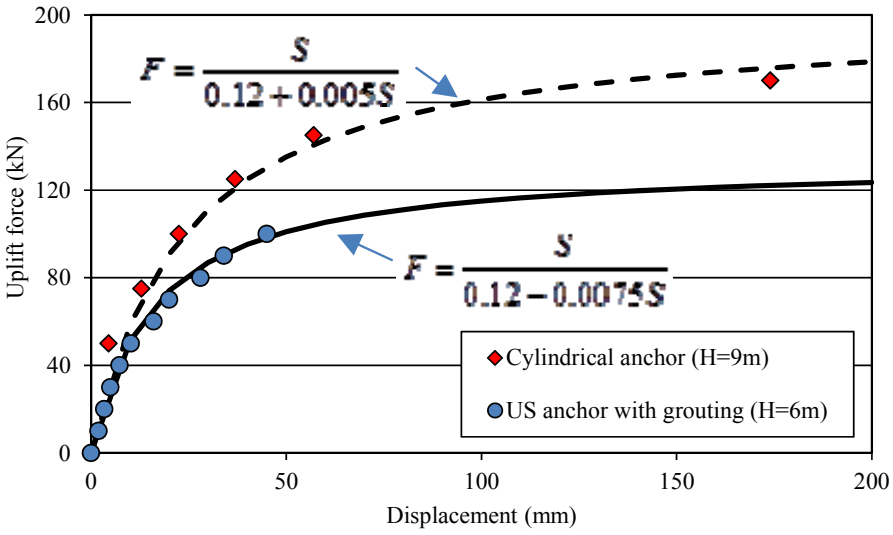


Fig. 10 Relationship between uplift force and displacement in the field uplift tests

the uplift test results of the US anchors of 6 m embedment depth ($H/D$ = 9.0). After the uplift displacement exceeded 50 mm, some of the displacement results were lost owing to a malfunction of the data acquisition system. The results from a cement grouted cylindrical anchor of 9 m embedment depth in the same site are also shown for comparison. The boreholes of these anchors are all 300 mm in diameter. It is found that the load-displacement relationships of these two types of anchors can be fitted by hyperbolic functions. Under the same test condition, the US anchor has shown satisfactory uplift capacity though its embedment depth was much smaller than the cylindrical anchor.

## 5. Numerical analyses

### *5.1 Finite element model*

In order to get a better understanding of the uplift behavior of the US ground anchor, a finite element model was established using ABAQUS program, a popular finite element program for geotechnical analysis (ABAQUS 2004). This commercial program has shown powerful and robust capabilities in nonlinear analysis. In the following numerical analyses, the US anchor has the dimensions of: $H$ = 6 m, $h$ = 1 m, $D$ = 650 mm, and $d$ = 160 mm, as shown in Fig. 11. The anchor body shown in Fig. 12 is assumed to be elastic and homogenous, and the Mohr-Coulomb elastic-plastic constitutive model is used to describe the stress-strain relationship of soil. The uplift condition of the vertically installed anchor is set to be axial symmetrical and rollers are used as the boundary constraint condition. The interface between the soil and the anchor is modelled using a pure master-slave surface contact element. The interface friction coefficient is set to be 0.3. The other parameters used in the numerical analyses are shown in Table 4. A sensitivity study on mesh density was conducted prior to the numerical investigation to ensure the finite element results are reliable.

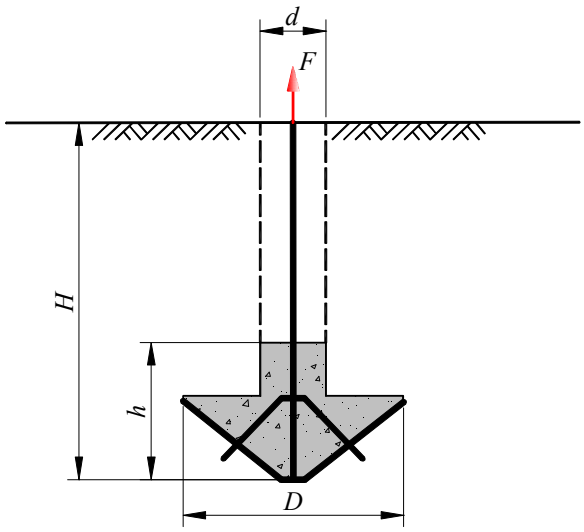


Fig. 11 Dimension diagram of the US ground anchor

Table 4 Parameters used in the numerical analyses

| Name | Unit weight $\gamma$ (kN/m$^3$) | Elastic modulus $E$ (MPa) | Poisson's ratio $v$ | Cohesion $c$ (kPa) | Friction angle $\varphi$ (°) |
|---|---|---|---|---|---|
| US anchor | 25 | 30000 | 0.167 | - | - |
| Steel rope | 78 | 200000 | 0.20 | - | - |
| Soil | 17.5 | 5 | 0.35 | 8.0 | 10.0 |

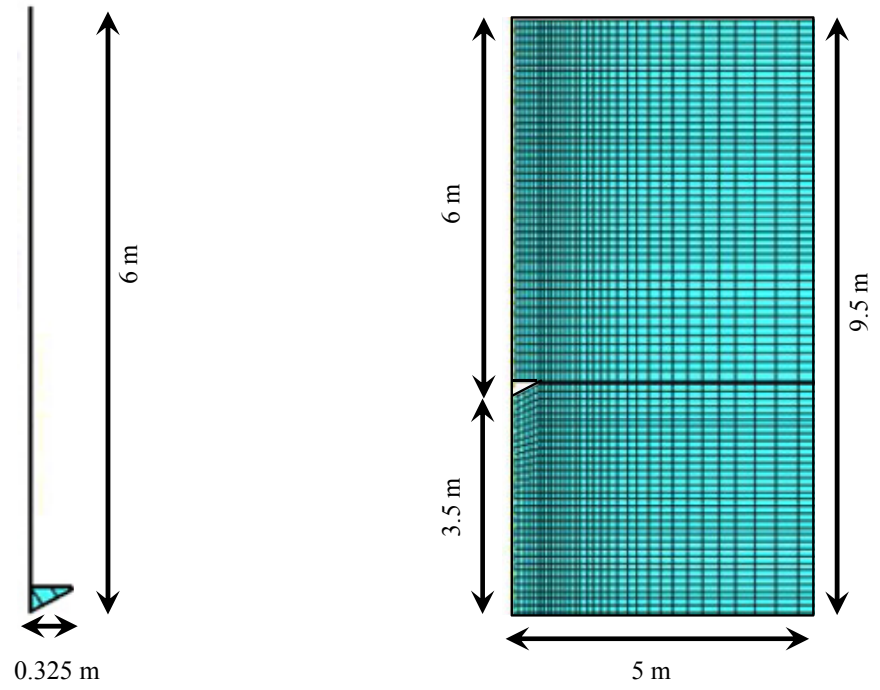


(a) US anchor (b) Ground soil

Fig. 12 Finite element model in the numerical analyses

Fig. 13 shows the contours of plastic strain in the ground soil during the pullout of the US anchor buried at 6 m depth, which clearly demonstrates the development of a plastic zone in soil mass around the anchor. Under the increased uplift loading, yielding of soil occurs and develops rapidly around the anchor head. The plastic zone expands upward with the increase of uplift loading, indicating an arc failure surface. It is found that the size of the plastic zone depends on the anchor diameter. The failure mode of this deep anchor can be characterized by localized yielding around the US anchor.

### *5.2 Parametric study*

The established numerical model was used to study the effect of the following parameters on the anchorage performance: (1) diameter of the anchor head $D$; (2) embedment depth $H$; (3) elastic

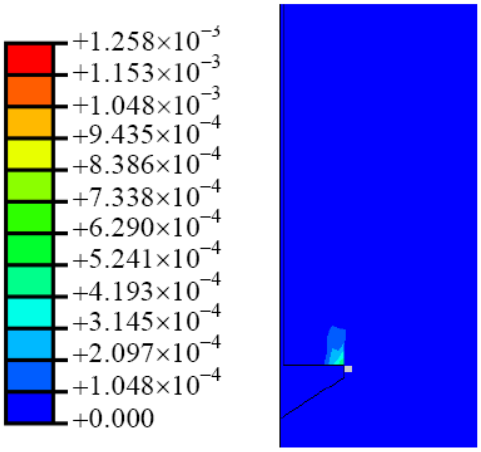


(a) Uplift force = 40 kN

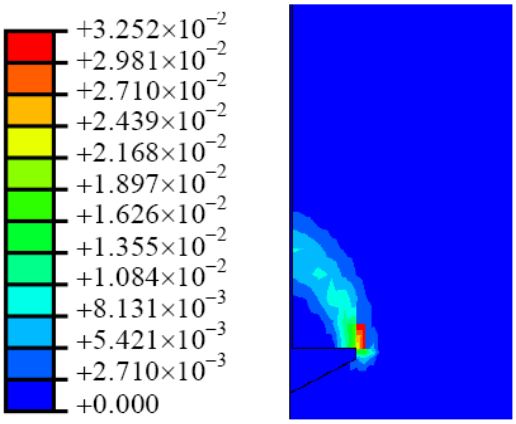


(b) Uplift force = 80 kN

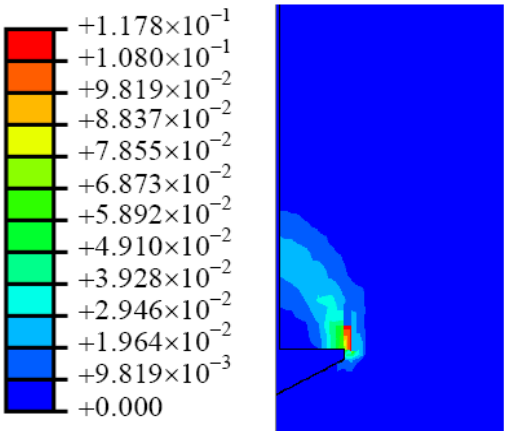


(c) Uplift force = 120 kN

Fig. 13 Contours of plastic strain in soil around the US anchor during pullout

modulus of soil $E$; (4) shear strength parameters of soil, including cohesion $c$ and friction angle $\varphi$. In the following parametric study, only one of the parameters was varied and the others are kept unchanged.

### *5.2.1 Effect of diameter of the anchor head*

The shape and size of the enlarged anchor head directly determine the magnitude of uplift capacity. Therefore, the anchor diameter is the key parameter that characterizes the expansion of the anchor size. A parameter study is conducted to explore the effect of anchor diameter on the uplift capacity with the fixed embedment depth and grouting height. The simulation results are shown in Fig. 14. According to the numerical results, with the increase in diameter, the ultimate uplift capacity of the US anchor has improved greatly, while the corresponding uplift displacement also increases significant. To perform a rationale design, the ultimate bearing capacity of the US anchor should be determined based on displacement criterion.

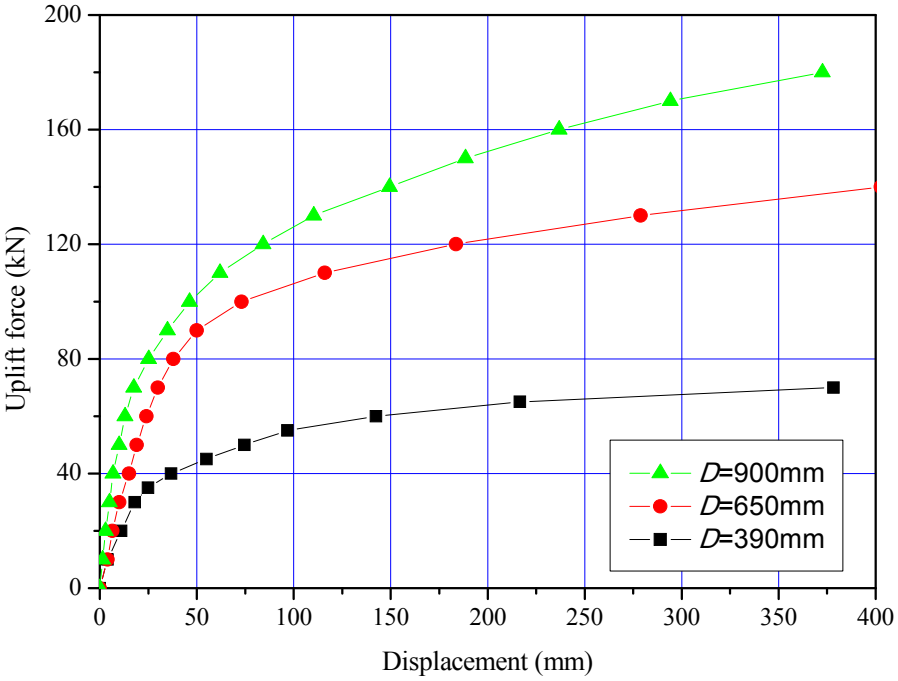


Fig. 14 Relationship between uplift force and displacement under different anchor diameters

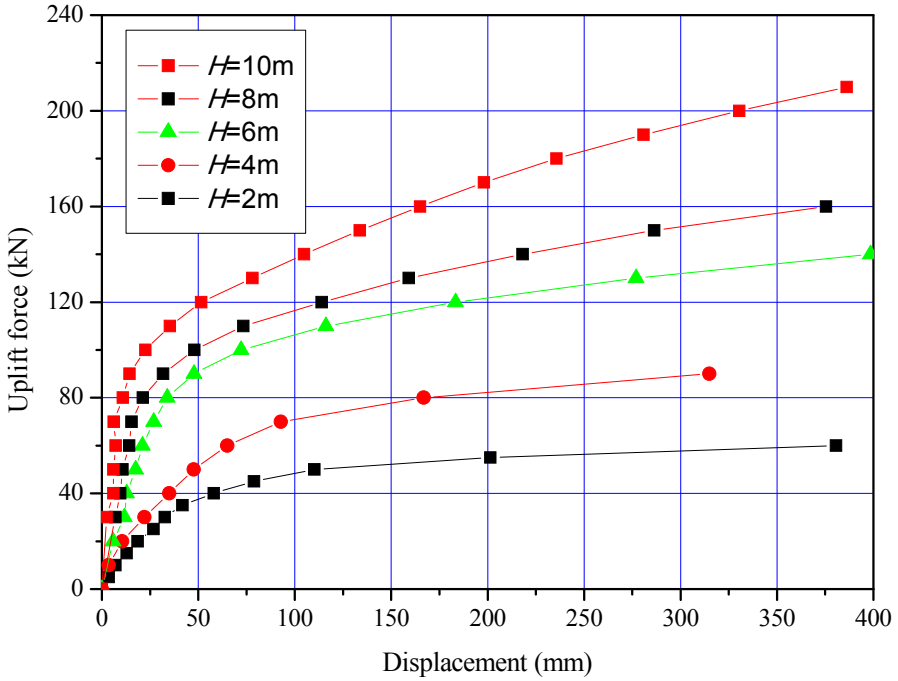


Fig. 15 Relationship between uplift force and displacement under different embedment depths

### 5.2.2 Effect of embedment depth

It has been demonstrated by numerous researches that the embedment depth is one of the crucial factors governing the uplift behavior of ground anchors. In this parametric study, the embedment cond depth is set to be 2, 4, 6, 8, 10 m, respectively. The simulation results are shown in Fig. 15. It is found that, for a certain uplift displacement, the uplift capacity increases with the increase of embedment depth. A greater embedment depth can provide better anchorage. However, the properties of the anchor material, the geological ition of the site, and construction feasibility should be taken into consideration when designing an appropriate embedment depth.

### 5.2.3 Effect of elastic modulus of soil

Besides the dimension of the ground anchor, the mechanical properties of ground soil also affect the uplift capacity. In this study, the elastic modulus of soil is set to be 1, 5, 10, 15, 20, 25 MPa, respectively. The simulation results in Fig. 16 show that, the influence of elastic modulus of soil on uplift behavior depends on the magnitude of soil stiffness. When the elastic modulus of soil is small, the increase of elastic modulus will dramatically improve the uplift capacity. When the elastic modulus is larger than 10 MPa, this effect is weakened.

### 5.2.4 Effect of soil shear strength

The uplift capacity of the US ground anchor should be highly dependent on the shear strength of ground soil. By adjusting the cohesion of soil from 10 to 40 kPa and friction angle from 10° to 40°, the influences of cohesion and friction angle of soil on the uplift behavior are investigated. It is found in Fig. 17 that when the uplift loading is in a small range, the increase in soil strength

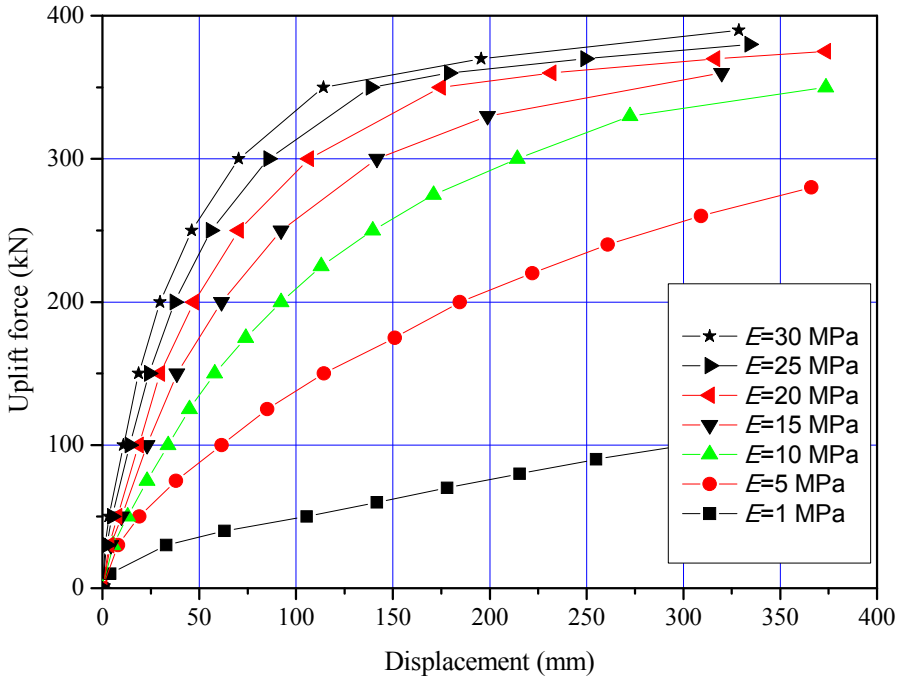


Fig. 16 Relationship between uplift force and displacement under different soil elastic moduli

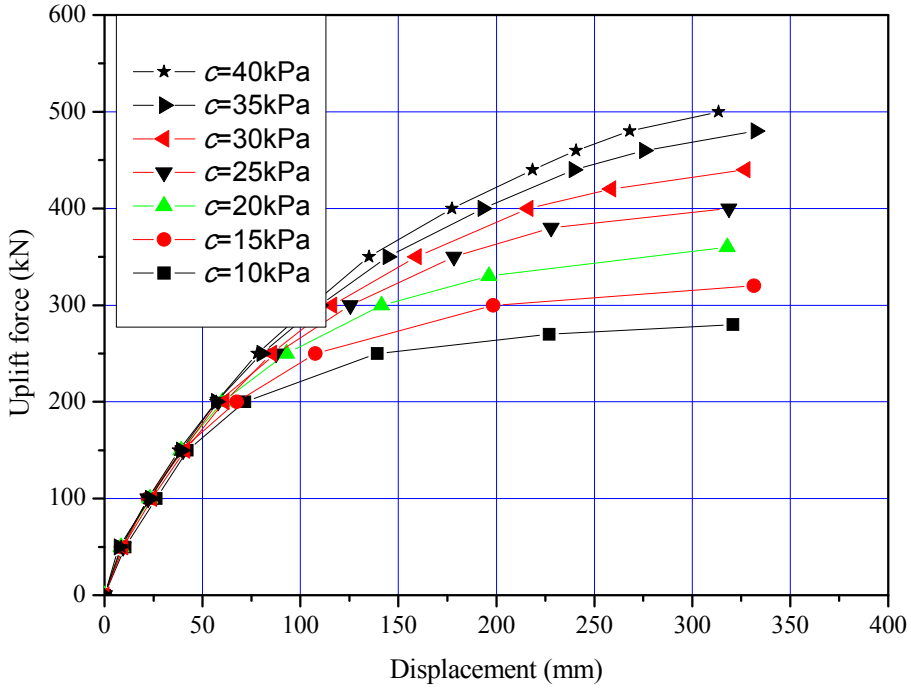


(a) Influence of cohesion

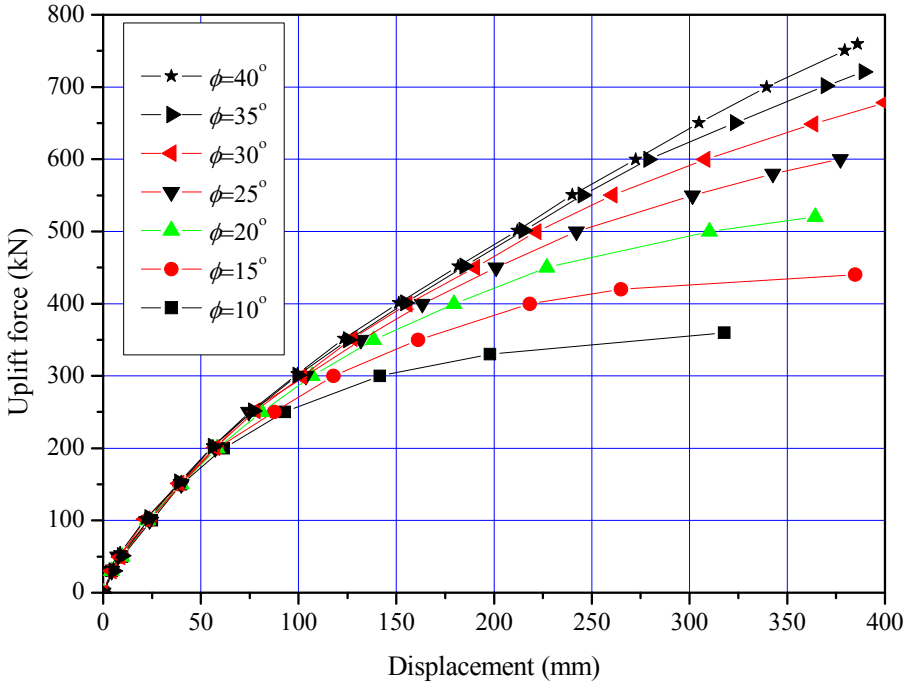


(b) Influence of friction angle

Fig. 17 Relationship between uplift force and displacement under different soil strength parameters

parameters will not affect the load-displacement relationship. The ultimate uplift capacity will be improved slightly if the cohesion and the friction angle become larger. It can be concluded that the increase of shear strength parameters of the bearing stratum can improve the uplift capacity to some content.

## 6. Conclusions

In this paper, a new type of underreamed ground anchors, that is, the umbrella-shaped anchors, is introduced. The uplift behavior of this anchor is studied through experimental and numerical analyses. The following conclusions are drawn based on the study:

(1) According to the laboratory and field uplift test results, the US anchor has a more satisfactory uplift capacity than conventional anchors. The load-deformation behavior of the US anchor can be described by a hyperbolic relationship.
(2) The failure mode of a deeply embedded US anchor can be characterized by an arc failure surface and the yielding zone extends some distance away below the ground surface. The size of the plastic zone is closely related to the anchor diameter.
(3) The anchor diameter and embedment depth have significant influence on the uplift behavior of the US anchor. The increase in anchor diameter and embedment depth will effectively improve the uplift capacity.
(4) The elastic modulus, cohesion, and friction angle of soil affect the uplift capacity to some content. In engineering design, soils with a stiffer modulus and larger shear strength are suggested to be selected as the bearing stratum of the umbrella-shaped anchor.

## Acknowledgments

The authors gratefully acknowledge the financial support provided by the National Natural Science Foundation of China (Nos. 41230636, 41302217, 51322807) and the National Basic Research Program of China (973 Program) (Grant No. 2011CB710605).

## References

ABAQUS, Inc. (2004), ABAQUS Analysis User's Manual, Version 6.4, Pawtucket, Rhode Island.

Bhattacharya, P. and Kumar, J. (2013), "Horizontal pullout capacity of a group of two vertical plate anchors in clay", *Geomech. Eng., Int. J.*, **5**(4), 299-312.

Consoli, N.C., Ruver, C.A. and Schnaid, F. (2013), "Uplift performance of anchor plates embedded in cement-stabilized backfill", *J. Geotech. Geoenviron. Eng. – ASCE*, **139**(3), 511-517.

Ghaly, A. and Hanna, A. (1994), "Ultimate pullout resistance of single vertical anchors", *Can. Geotech. J.*, **31**(5), 661-672.

Hong, C.Y., Yin, J.H., Zhou, W.H. and Pei, H.F. (2012), "Analytical study on progressive pullout behavior of a soil nail", *J. Geotech. Geoenviron. Eng. – ASCE*, **138**(4), 500-507.

Hong, C.Y., Yin, J.H. and Pei, H.F. (2013a), "Comparative study on the pullout behaviour of pressure grouted soil nails from field and laboratory tests", *J. Cent. South Univ.*, **20**(8), 2285-2292.

Hong, C.Y., Yin, J.H., Pei, H.F. and Zhou, W.H. (2013b), "Experimental study on the pullout resistance of pressure grouted soil nails in the field", *Can. Geotech. J.*, **50**(7), 693-704.

Huang, F., Yang, X.L. and Huang, K. (2011), "Upper bound solution of ultimate pullout capacity of strip plate anchor subjected to pore pressure based on Hoek-Brown failure criterion", *Adv. Mater. Res.*, **255-260**, 146-150.
Hsu, S.T. and Liao, H.J. (1998), "Uplift behavior of cylindrical anchors in sand", *Can. Geotech. J.*, **34**(1), 70-80.
Ilamparuthi, K., Dickin, E.A. and Muthukrisnaiah, K. (2002), "Experimental investigation of the uplift behaviour of circular plate anchors embedded in sand", *Can. Geotech. J.*, **39**(3), 648-664.
Kame, G.S., Dewaikar, D.M. and Choudhury, D. (2012), "Pullout capacity of vertical plate anchors in cohesion-less soil", *Geomech. Eng., Int. J.*, **4**(2), 105-120.
Liao, H.J. and Hsu, S.T. (2003), "Uplift behavior of blade-underreamed anchors in silty sand", *J. Geotech. Geoenviron. Eng. – ASCE*, **129**(6), 79-95.
Liu, H., Wang, C. and Zhao, Y. (2013), "Analytical study of the failure mode and pullout capacity of suction anchors in clay", *Ocean Syst. Eng., Int. J.*, **3**(2), 187-194.
Liu, Y., Mei, G.X., Song, L.H. and Zai, J.M. (2009), "Manufacture and experimental study of a new type umbrella-shaped anti-float anchor", *Chin. J. Rock Mech. Eng.*, **28**(1), 2935-2940. [In Chinese]
Matsuo, M. (1967), "Study of uplift resistance of footings: I", *Soils Found.*, **7**(4), 1-37.
Matsuo, M. (1968), "Study of uplift resistance of footings: II", *Soils Found.*, **8**(1), 18-48.
Merfield, R.S., Lyamin, A.V., Sloan, S.W. and Yu, H.S. (2003), "Three-dimensional lower bound solutions for stability of plate anchors in clay", *J. Geotech. Geoenviron. Eng. – ASCE*, **129**(3), 243-253.
Murray, E.J. and Geddes, J.D. (1987), "Uplift behaviour of anchor plates in sand", *J. Geotech. Eng. – ASCE*, **113**(3), 202-215.
Niroumand, H. and Kassim, K.A. (2013), "A review on uplift response of symmetrical anchor plates embedded in reinforced sand", *Geomech. Eng., Int. J.*, **5**(3), 187-194.
Rowe, R.K. and Davis, E.H. (1982a), "The behavior of anchor plates in clay", *Geotechnique*, **32**(1), 9-23.
Rowe, R.K. and Davis, E.H. (1982b), "The behavior of anchor plates in sand", *Geotechnique*, **32**(1), 25-41.
Singh, S.P. and Ramaswamy, S.V. (2008), "Effect of shape on holding capacity of plate anchors buried in soft soil", *Geomech. Geoeng.*, **3**(2), 157-166.
Xu, M., Song, L.H., Zhou, F., Mei, G.X. and Zai, J.M. (2009), "In-situ test and numerical simulation of the umbrella-shaped uplift anchor", *Rock Soil Mech.*, **30**(S), 24-28. [In Chinese]
Yin, J.H. and Zhou, W.H. (2009), "Influence of grouting pressure and overburden stress on the interface resistance of a soil nail", *J. Geotech. Geoenviron. Eng. – ASCE*, **135**(9), 1198-1208.
Zhang, J.H. (2006), "Study on effect of umbrella-shaped self-expanding anchor after its application", *Rock Soil Mech.*, **27**(5), 842-845. [In Chinese]
Zhang, C.C., Xu, Q, Zhu, H.H., Shi, B. and Yin, J.H. (2014), "Evaluations of load-deformation behavior of soil nail using hyperbolic pullout model", *Geomech. Eng., Int. J.*, **6**(3), 277-292.
Zhou, W.H. and Yin, J.H. (2008), "A simple mathematical model for soil nail and soil interaction analysis", *Comput. Geotech.*, **35**(3), 479-488.
Zhou, W.H., Yin, J.H. and Hong, C.Y. (2011), "Finite element modelling of pullout testing on a soil nail in a pullout box under different overburden and grouting pressures", *Can. Geotech. J.*, **48**(4), 557-567.
Zhou, W.H., Yuen, K.V. and Tan, F. (2013), "Estimation of maximum pullout shear stress of grouted soil nails using Bayesian probabilistic approach", *Int. J. Geomech. – ASCE*, **13**(5), 659-664.
Zhu, H.H., Yin, J.H., Yeung, A.T. and Jin, W. (2011), "Field pullout testing and performance evaluation of GFRP soil nails", *J. Geotech. Geoenviron. Eng. – ASCE*, **137**(7), 633-641.

*CC*